

MODELING CONTAMINANT MIGRATION WITH LINEAR SORPTION IN STRONGLY HETEROGENEOUS MEDIA

By M. Bai,¹ D. Elsworth,² Member, ASCE, H. I. Inyang,³ Member, ASCE, and J.-C. Roegiers⁴

ABSTRACT: A triple-porosity model is presented to evaluate transport behavior in porous media with a structure comprising a spectrum of pore sizes, represented discretely as macro-, meso-, and micropores. Characterizations are completed to provide adequate semianalytical solutions for the validation of codes representing discrete distributions of pore geometry and to adequately describe extended tailing and multicomponent solute front breakthroughs apparent in field and laboratory data. Semianalytical solutions are derived for a one dimensional flow geometry by using Laplace transforms under the assumption that solute transport in the two interactive mobile-transport regions (i.e., macro- and mesopores) is affected by exchange with immobile solutes in the micropore region. Sensitivity analyses are conducted to identify the propensity for extensive tailing in the breakthrough response, over single-porosity approaches, and the development of multiple breakthrough fronts with reverse diffusion. Both behaviors result from the strongly heterogeneous nature of the transport processes, accommodated in the multiporosity model, and are well suited to the representation of "real" porous and porous-fractured disordered media.

INTRODUCTION

Porous media commonly exhibit heterogeneities at a variety of scales, including cracks, fractures, interconnected macropores, and aggregate micropores, all of which may result in the development of dynamic instabilities of the wetting front during fluid infiltration (Gerke and van Genuchten 1993). These structures, at varying length scales, and the resulting flow processes frequently affect solute migration at the macroscopic level by creating nonuniform flow fields with substantial velocity contrasts. When these spatial variabilities are prevalent, the effects of the heterogeneities must be characterized and incorporated into the modeling if an accurate description of behavior is sought.

To match the nonuniform pressure or concentration profiles observed in the laboratory and field, the use of dual-porosity models to characterize behavior has become popular. Such an approach assumes that porous media consist of two regions with distinct flow properties. Macropores, or fractures, form preferential flow channels, whereas less permeable soil aggregates or rock matrix blocks act as branched flow paths connected to the main channels (Barenblatt et al. 1960). These branch-flow paths assist either in reducing mass fluxes within channels by direct diversion or in replenishing the channels with additional stored mass, depending upon the pressure (or concentration) gradients between the two regions (Bai et al. 1996). Through restricting mass transfer within the rock matrix or micropores, simpler but more practical dual-porosity models were developed by Warren and Root (1963) for fluid flow and by Coats and Smith (1964) for solute transport. The "compartment model" by the former and the "capacitance model" by the latter are applicable only to the scenario where the hydrological properties between the primary channels and branch paths are significantly different. Errors, particularly at

early times, are accentuated if the difference is substantially reduced (Chen 1989).

With respect to mass transport, a further complication is associated not only with the physical interplay between macro- and micropores, but also with the interplay between dispersion and convection, as characterized by Péclet number. Nonuniform solute transport in soils has been observed in many experiments in the form of early breakthrough and extended tailing (Anderson 1979). This behavior is typically ascribed to physical reasons, including the prevalence of anisotropic hydraulic conductivities, heterogeneous soil structures, and non-equilibrium sorption characteristics (Brusseu and Rao 1990). Theoretically, this nonuniform behavior may become prominent through increasing the ratio between flow velocity and dispersion coefficient, as embodied within the Péclet number. Considering the physics behind this explanation of behavior, the nonuniform response in the concentration field is attributed to the influence of velocity variations at the micropore level (Passioura 1971; Li et al. 1994).

The use of a dual-porosity approach to represent transport behavior (envisioning two regions, e.g., mobile and immobile regions) may be insufficient to characterize highly heterogeneous porous media containing pore structures at a variety of length scales. In this, mesopores of intermediate scale may exist as a buffer zone to modify mass transfer between macropores and micropores. Characteristic response of a triple-porosity medium yields a spectrum of breakthrough curves, typically with enhanced tailing (Abdassah and Ershaghi 1986; Bai et al. 1993). As pointed out by Gwo et al. (1996), it is appropriate to view soils as consisting of a continuous distribution of pore sizes that may be segregated into macro-, meso-, and micropore regions, analogous to particle-size distribution being segregated into sand, silt, and clays. Luxmoore et al. (1990) defined macropores and micropores as pores with "equivalent pore diameters" (EPD) greater than 1 mm and less than 0.01 mm, respectively. Gwo et al. (1995) alternatively divided the pore structures into three regions by adding a mesopore region with a corresponding EPD between 0.01 mm and 1 mm.

Examination of the triple-porosity behavior of porous media may not only provide a rationale to replicate the complex physical phenomena related to transport in heterogeneously structured soils, but also suggest an alternative tool in matching unusual response in physical experiments. As illustrated in Fig. 1, a structured soil may be divided into three distinct porous domains (macro-, meso-, and micropores) that may be alternately envisioned as consisting of fractures, microfractures, and matrix pores with three different velocity and dis-

¹Res. Assoc., Rock Mechanics Inst., Univ. of Oklahoma, Norman, OK 73019.

²Prof., Dept. of Mineral Engrg., Pennsylvania State Univ., University Park, PA 16802.

³Assoc. Prof., Dept. of Civ. and Envir. Engrg., Univ. of Massachusetts, Lowell, MA 01854.

⁴Dir. and Prof., Rock Mechanics Inst., Univ. of Oklahoma, Norman, OK.

Note. Associate Editor: Dr. Susan E. Powers. Discussion open until April 1, 1998. To extend the closing date one month, a written request must be filed with the ASCE Manager of Journals. The manuscript for this paper was submitted for review and possible publication on January 8, 1997. This paper is part of the *Journal of Environmental Engineering*, Vol. 123, No. 11, November, 1997. ©ASCE, ISSN 0733-9372/97/0011-1116-1125/\$4.00 + \$.50 per page. Paper No. 14896.

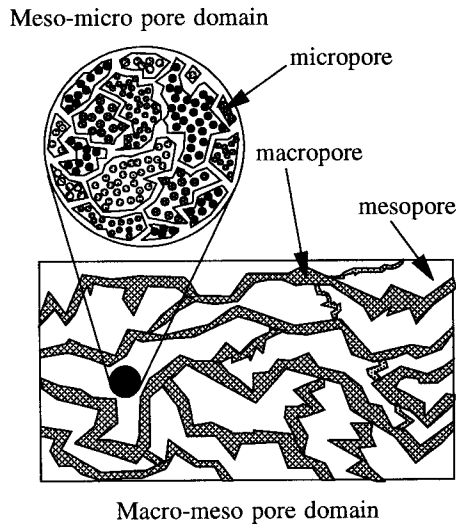


FIG. 1. Schematic Triple-Porosity Scenario

persion profiles. While macropores act as preferential channels for mass transport, mesopore regions are considered as branch paths to divert solute either out from or into the least permeable micropore aggregates. Compared with traditional dual-porosity conceptualization (Bai and Elsworth 1995) this cascading or "tree" structured triple-porosity model leads to a refined classification of transport domains in terms of their temporal and spatial scales. In contrast to other triple-porosity models [e.g., Bai and Roegiers (1996, in press)], the present model preserves the mechanism of complete hydrodynamic dispersion in mesopores, while adding linear sorption to all porous spaces in an effort to encompass the critical fluid-solid retardation process in the analysis. This increases the versatility of modeling and the fidelity with which real behavior may be matched. Correspondingly, an improved triple-porosity model is proposed and presented in the following section, together with semianalytical solutions for one dimensional (1D) solute transport.

MATHEMATICAL FORMULATION

Assuming constant porosity, defining an average velocity for each porous space v ($v = v^*/n$, v^* is the intrinsic interstitial velocity), requiring that the quasisteady mass exchange rate is proportional to the concentration gradients among the three continua (Bear 1972; Bai et al. 1993; Gwo et al. 1995), and considering linear sorption for the low liquid-concentration range (Ogata 1964), the general governing equations for solute transport in a triple-porosity system can be described as

$$\frac{\partial}{\partial x_i} \left(D_{mij} \frac{\partial c_m}{\partial x_j} \right) - v_{mi} \frac{\partial c_m}{\partial x_i} = \frac{\partial c_m}{\partial t} + \frac{\xi_{mm_1}}{n_m} (c_m - c_{m_1}) + \frac{\xi_{mm_2}}{n_m} (c_m - c_{m_2}) + \frac{\partial \sigma_m}{\partial t} \quad (1)$$

$$\frac{\partial \sigma_m}{\partial t} = K_{pm}(c_m - \epsilon_m \sigma_m) \quad (2)$$

where subscripts 1, 2, and 3 = macro-, meso-, and micropores, respectively; subscripts m , m_1 , and m_2 follow rotational order (i.e., $m = 1, 2, 3$; $m_1 = 2, 3, 1$; and $m_2 = 3, 1, 2$); subscripts i and j = coordinate indices; c = solute concentration; t = time after inception of transport; x_i = coordinate; D_{ij} = hydrodynamic dispersion tensor; v_i = average flow velocity; n = porosity; ξ = a concentration exchange coefficient characterizing mass transfer between pores at various scales; σ = function of sorption isotherm that is represented by the product of solid-

phase density and sorbed mass per unit mass of solids over the porosity; K_p = sorption intensity factor; and ϵ = process factor signaling whether the process is irreversible ($\epsilon = 0$) or can be reversible (e.g., $\epsilon \sigma > c$).

From governing equations (1) and (2), it is seen that contaminant migration can be attenuated not only by the transient mass storage variations, including mass exchange among pore spaces of various scales, but also by irreversible adsorption, or reversible desorption (sorption as a whole). As a surrogate for chemical reactions, the sorption mechanism is defined as the removal or addition of contaminant by the solid matrix through which the fluid flows. For example, sorption reactions remove contaminants from ground water and add them to the surfaces of minerals or the solid organic carbon of the unit through which the contaminants are moving (Water Science and Technology Board 1990). When sorption occurs, the rate of contaminant migration is lower than the case for an unretarded or neutral tracer. This behavior helps to reduce the spread of contaminants but also provides a dormant source that may be reactivated later as aqueous concentration declines and the sorption process reverses.

Eq. (1) can be simplified by using the assumptions that (1) Direct solute exchange between macropores and micropores is insignificant; (2) solute within micropores is immobile (Coats and Smith 1964); (3) the dispersion coefficient D is constant; and (4) solute transport is 1D. As a result, Eq. (1) in an expanded form becomes

$$D_1 \frac{\partial^2 c_1}{\partial x^2} - v_1 \frac{\partial c_1}{\partial x} = \frac{\partial c_1}{\partial t} + \frac{\xi_{12}}{n_1} (c_1 - c_2) + \frac{\partial \sigma_1}{\partial t} \quad (3)$$

$$D_2 \frac{\partial^2 c_2}{\partial x^2} - v_2 \frac{\partial c_2}{\partial x} = \frac{\partial c_2}{\partial t} + \frac{\xi_{21}}{n_2} (c_2 - c_1) + \frac{\xi_{23}}{n_2} (c_2 - c_3) + \frac{\partial \sigma_2}{\partial t} \quad (4)$$

$$0 = \frac{\partial c_3}{\partial t} + \frac{\xi_{32}}{n_3} (c_3 - c_2) + \frac{\partial \sigma_3}{\partial t}; \quad \frac{\partial \sigma_1}{\partial t} = K_{p1}(c_1 - \epsilon_1 \sigma_1) \quad (5, 6)$$

$$\frac{\partial \sigma_2}{\partial t} = K_{p2}(c_2 - \epsilon_2 \sigma_2); \quad \frac{\partial \sigma_3}{\partial t} = K_{p3}(c_3 - \epsilon_3 \sigma_3) \quad (7, 8)$$

For more general solution, the following dimensionless terms are introduced:

$$y = \frac{x}{L}, \quad \tau = \frac{v_1 t}{L}, \quad \gamma_i = \frac{v_i L}{D_i}, \quad b_i = \frac{v_i}{v_1}, \quad a_{ij} = \frac{\xi_{ij} L}{n_i v_1}, \quad \eta_i = \frac{L}{v_1} K_{pi} \quad (9)$$

where subscripts $i = 1, 2, 3$; $j = 1, 2, 3$ but $i \neq j$; $i = 1$ and 2 for γ_i and b_i only; and L = an arbitrary length that may represent sample or domain length. Because b_1 is always equal to 1, it is omitted in the following formation.

Incorporating all dimensionless terms, (3)–(8) are rewritten as

$$\frac{1}{\gamma_1} \frac{\partial^2 c_1}{\partial y^2} - \frac{\partial c_1}{\partial y} = \frac{\partial c_1}{\partial \tau} + a_{12}(c_1 - c_2) + \frac{\partial \sigma_1}{\partial \tau} \quad (10)$$

$$\frac{1}{\gamma_2} \frac{\partial^2 c_2}{\partial y^2} - \frac{\partial c_2}{\partial y} = b_2 \left[\frac{\partial c_2}{\partial \tau} + a_{21}(c_2 - c_1) + a_{23}(c_2 - c_3) + \frac{\partial \sigma_2}{\partial \tau} \right] \quad (11)$$

$$0 = \frac{\partial c_3}{\partial \tau} + a_{32}(c_3 - c_2) + \frac{\partial \sigma_3}{\partial \tau}; \quad \frac{\partial \sigma_1}{\partial \tau} = \eta_1(c_1 - \epsilon_1 \sigma_1) \quad (12, 13)$$

$$\frac{\partial \sigma_2}{\partial \tau} = \eta_2(c_2 - \epsilon_2 \sigma_2); \quad \frac{\partial \sigma_3}{\partial \tau} = \eta_3(c_3 - \epsilon_3 \sigma_3) \quad (14, 15)$$

For step injection at the inlet and constant flux (zero flux for this case) at the outlet, boundary and initial conditions may be described by

$$c_1 = c_2 = c^0 \quad (y = 0); \quad \frac{\partial c_1}{\partial y} = \frac{\partial c_2}{\partial y} = 0 \quad (y = 1) \quad (16a,b)$$

$$c_1 = c_1^0, \quad c_2 = c_2^0, \quad c_3 = c_3^0 \quad (\tau = 0) \quad (16c)$$

$$\sigma_1 = \sigma_1^0, \quad \sigma_2 = \sigma_2^0, \quad \sigma_3 = \sigma_3^0 \quad (\tau = 0) \quad (16d)$$

where c^0 = concentration at the source; c_1^0 , c_2^0 , and c_3^0 = initial concentrations; and σ_1^0 , σ_2^0 , and σ_3^0 = initial sorbent concentrations in macro-, meso-, and micropores, respectively. The field equations and boundary conditions, represented in (10)–(16), are applicable to solute injection within a finite column of triple-porosity medium.

Applying a Laplace transform to (10)–(15) yields

$$\frac{1}{\gamma_1} \frac{d^2 \bar{c}_1}{dy^2} - \frac{d\bar{c}_1}{dy} = s\bar{c}_1 - c_1^0 + a_{12}(\bar{c}_1 - \bar{c}_2) + s\bar{\sigma}_1 - \sigma_1^0 \quad (17)$$

$$\frac{1}{\gamma_2} \frac{d^2 \bar{c}_2}{dy^2} - \frac{d\bar{c}_2}{dy} = b_2[(s\bar{c}_2 - c_2^0) + a_{21}(\bar{c}_2 - \bar{c}_1) + a_{23}(\bar{c}_2 - \bar{c}_3) + s\bar{\sigma}_2 - \sigma_2^0] \quad (18)$$

$$0 = s\bar{c}_3 - c_3^0 + a_{32}(\bar{c}_3 - \bar{c}_2) + s\bar{\sigma}_3 - \sigma_3^0 \quad (19)$$

$$s\bar{\sigma}_1 - \sigma_1^0 = \eta_1(\bar{c}_1 - \varepsilon_1 \bar{\sigma}_1) \quad (20)$$

$$s\bar{\sigma}_2 - \sigma_2^0 = \eta_2(\bar{c}_2 - \varepsilon_2 \bar{\sigma}_2); \quad s\bar{\sigma}_3 - \sigma_3^0 = \eta_3(\bar{c}_3 - \varepsilon_3 \bar{\sigma}_3) \quad (21, 22)$$

where s is the Laplace transform parameter.

Boundary conditions in the Laplace domain are transformed as

$$\bar{c}_1 = \bar{c}_2 = \frac{c^0}{s} \quad (y = 0); \quad \frac{d\bar{c}_1}{dy} = \frac{d\bar{c}_2}{dy} = 0 \quad (y = 1) \quad (23a,b)$$

The relationship between $\bar{\sigma}_i$ and \bar{c}_i ($i = 1, 2, 3$) can be derived from (20)–(22). The subsequent results can be substituted into (17)–(19) to eliminate unknowns $\bar{\sigma}_i$ ($i = 1, 2, 3$). As a result, (17)–(22) reduce to

$$\frac{1}{\gamma_1} \frac{d^2 \bar{c}_1}{dy^2} - \frac{d\bar{c}_1}{dy} = s\bar{c}_1 - c_1^0 + a_{12}(\bar{c}_1 - \bar{c}_2) + \eta_1^* \bar{c}_1 + \eta_1^0 \quad (24)$$

$$\frac{1}{\gamma_2} \frac{d^2 \bar{c}_2}{dy^2} - \frac{d\bar{c}_2}{dy} = b_2[(s\bar{c}_2 - c_2^0) + a_{21}(\bar{c}_2 - \bar{c}_1) + a_{23}(\bar{c}_2 - \bar{c}_3)] + \eta_2^* \bar{c}_2 + \eta_2^0 \quad (25)$$

$$0 = s\bar{c}_3 - c_3^0 + a_{32}(\bar{c}_3 - \bar{c}_2) + \eta_3^* \bar{c}_3 + \eta_3^0 \quad (26)$$

where

$$\eta_1^* = \frac{s\eta_1}{s + \eta_1\varepsilon_1}; \quad \eta_2^* = \frac{sb_2\eta_2}{s + \eta_2\varepsilon_2}; \quad \eta_3^* = \frac{s\eta_3}{s + \eta_3\varepsilon_3} \quad (27)-(29)$$

$$\eta_1^0 = \sigma_1^0 \left(\frac{s}{s + \eta_1\varepsilon_1} - 1 \right); \quad \eta_2^0 = b_2\sigma_2^0 \left(\frac{s}{s + \eta_2\varepsilon_2} - 1 \right) \quad (30, 31)$$

$$\eta_3^0 = \sigma_3^0 \left(\frac{s}{s + \eta_3\varepsilon_3} - 1 \right) \quad (32)$$

The relationship between \bar{c}_2 and \bar{c}_3 can be derived from (26) as

$$\bar{c}_3 = \frac{c_3^0 + a_{32}\bar{c}_2 - \eta_3^0}{s + a_{32} + \eta_3^*} \quad (33)$$

Substituting (33) into (25) results in

$$\frac{1}{\gamma_2} \frac{d^2 \bar{c}_2}{dy^2} - \frac{d\bar{c}_2}{dy} - \phi_{21}\bar{c}_2 = -b_2a_{21}\bar{c}_1 + \phi_{22} \quad (34)$$

where

$$\phi_{21} = b_2 \left(s + a_{21} + a_{23} - \frac{a_{23}a_{32}}{s + a_{32} + \eta_3^*} \right) + \eta_2^* \quad (35)$$

$$\phi_{22} = -b_2 \left[c_2^0 + \frac{a_{23}(c_3^0 - \eta_3^0)}{s + a_{32} + \eta_3^*} \right] + \eta_2^0 \quad (36)$$

Eq. (24) can be rewritten as

$$\frac{1}{\gamma_1} \frac{d^2 \bar{c}_1}{dy^2} - \frac{d\bar{c}_1}{dy} - \phi_{11}\bar{c}_1 = -a_{12}\bar{c}_2 + \phi_{12} \quad (37)$$

where

$$\phi_{11} = s + a_{12} + \eta_1^*; \quad \phi_{12} = -c_1^0 + \eta_1^0 \quad (38)$$

For brevity and completeness, the detailed analytical procedure and entire solutions of the coupled equations (37) and (34) are given in the Appendix. Once \bar{c}_2 is obtained, \bar{c}_1 and \bar{c}_3 can be derived from (42) in the Appendix and (33), respectively. Solute concentrations in the untransformed (natural) domain may be recovered through numerical inversion (Stehfest 1970). The solutions are most conveniently expressed in normalized form as c_i/c^0 where $i = 1, 2, 3$.

SENSITIVITY ANALYSIS

In addition to better replicate the behavior of structured porous media having multiple characteristic scales, one of the aims of developing a triple-porosity model is to provide a more flexible tool in predicting and matching actual measurements. In comparison with the traditional dual-porosity approach, this versatile tool can be examined through simple sensitivity analyses. As defined in the dimensionless groups of (9), principal parameters for the designated location y and time τ are as follows: (1) Equivalent Péclet number (EPN) γ_i ($i = 1, 2$) for macro- and mesopores; (2) solute exchange intensity factor a_{ij} ($ij = 12, 21, 23, 32$); (3) flow velocity ratio b_i ($i = 1, 2$); and (4) equivalent sorption intensity factor η_i ($i = 1, 2, 3$). The dimensionless initial solute concentrations $c_i^* = c_i^0/c^0$ and the process factors ε_i ($i = 1, 2, 3$) are predetermined for all porous phases as $c_1^* = 0.1$, $c_2^* = 0.3$, $c_3^* = 0.5$, $\varepsilon_1 = 0.1$, $\varepsilon_2 = 0.2$, and $\varepsilon_3 = 0.3$. All parameters are listed in Table 1 with corresponding figures. The dimensionless solid-phase concentrations listed in Table 1 are defined as $\sigma_i^* = \sigma_i^0/c^0$. In the

TABLE 1. Selected Dimensionless Parameters

Figure (1)	γ_1 (2)	γ_2 (3)	a_{12} (4)	a_{21} (5)	a_{23} (6)	a_{32} (7)	b_2 (8)	η_1 (9)	η_2 (10)	η_3 (11)	σ_1^* (12)	σ_2^* (13)	σ_3^* (14)
2	0.1–100	10	0.5	0.4	0.3	0.2	2	0.001	0.01	0.1	0.1	0.01	0.001
3	1–20	10	0	0.4	0.3	0.2	2	0	0.01	0.1	0	0.01	0.001
4a	20	10	0.1	0.05	0.01	0.005	2	0.001	0.01	0.1	0.1	0.01	0.001
4b	20	10	0.5	0.4	0.3	0.2	2	0.001	0.01	0.1	0.1	0.01	0.001
4c	20	10	1	0.8	0.6	0.4	2	0.001	0.01	0.1	0.1	0.01	0.001
5	20	10	0.5	0.4	0.3	0.2	2–50	0.001	0.01	0.1	0.1	0.01	0.001
6	20	10	0.5	0.4	0.3	0.2	2	0.001–0.5	0.01–0.6	0.1–0.7	0.1	0.01	0.001
7a	20	10	0	0.4	0.3	0.2	2	0	0.01	0.1	0	0.01	0.001
7b	20	10	0.5	0.4	0	0	2	0.001	0	0.1	0.1	0	0.001
7c	20	10	0.5	0.4	0.3	0.2	2	0.001	0.01	0.1	0.1	0.01	0.001
8	20	10	0.5	0.4	5	4	2	0.001	0.01	0.1	0.1	0.01	0.001

illustrated figures, the concentration relative to the maximum value at the injection point is referred to the quantity for macropores. The analysis is constrained to the study of temporal concentration changes (breakthrough) at a specified location ($y = 0.5$).

Determination of sensible parametric ranges for Table 1 may be through (1) Previous experimental data; (2) related literature search; and (3) physical intuition and judgment. Even though the grouped dimensionless parameters are used, reasonable magnitudes of original parameters still need to be considered and accommodated because the variation of one parameter may affect other parameters due to the chain relationships shown in (9). From the literature, certain general rules may be derived in view of the parametric ranges.

Among all parameters, EPN γ_i may be the most important to be defined because it relates to the reverse relationship between the flow velocity and the hydrodynamic dispersion. For the case of the "capacitance" concept, γ_i for the macropores is typically in the range 50–780 for the experimental setup by Coats and Smith (1964). However, the range may drop to 10–18 from the test data of Bouhroum and Bai (1996). The breakthrough profiles subjected to the limiting cases of γ in a single-porosity scenario can be obtained from Passioura (1971). In view of the relative magnitudes of velocity v_i and dispersion D_i ($i = 1, 2, 3$) for each porous phase, the general rules of $v_1 > v_2 > v_3$ and $D_1 < D_2 < D_3$ for the triple-porosity model can be found in Gwo et al. (1995). Applying the definition that $\gamma_i = v_i L / D_i$, it appears that $\gamma_1 > \gamma_2$ when L is a constant for the present case. However, these rules are not universal and exceptions should be permitted [e.g., $D_1 > D_2 > D_3$; also see Gwo et al. (1995)]. Due to the greater flow cross-sectional area for the larger pore phase, $v_1 > v_2$ (i.e., $b_2 > b_1$) for dual-porosity situations may be commonly defined (Gerke and van Genuchten 1993).

With regard to the solute exchange factor a_{ij} , a broad range is defined as 0.017–1.54 by Coats and Smith (1964), whereas this range is narrowed down to 0.34–0.59 by Bouhroum and Bai (1996). For the dimensional parameter ξ_{ij} , which is a concentration exchange coefficient, it is known that $\xi_{12} > \xi_{23}$ (Gwo et al. 1995). Using physical intuition and considering the principle of mass balance, the following equality results: $\xi_{12} = \xi_{21}$ and $\xi_{23} = \xi_{32}$. Based on the literature (Warren and Root 1963; Bai et al. 1993), larger conductivity media in general occupy a smaller volume (i.e., have smaller overall porosity) and one has $n_3 > n_2 > n_1$. As a result, and recalling that $a_{ij} = \xi_{ij} L / (n_i v_i)$, the following relationship becomes a natural consequence when L and v_i are held constant: $a_{12} > a_{21} > a_{23} > a_{32}$. Again, exceptions do exist.

Fewer references may be made to the parameters in sorption for multiporosity media. However, Mannhardt and Nasr-El-Din (1994) and Ogata (1964) indicated that sorption mechanisms act as a supplemental form of the capacitance effect in mobile and immobile zones proposed by Coates and Smith (1964). The parametric ranges for sorption are chosen based on both literature and physical intuition.

It should be emphasized that the following sensitivity study involves the change of one parameter at one time while other parameters are held constant with the consideration of the chain effect discussed earlier.

Fig. 2 depicts the effects of increasing the EPN of macropores (γ_1) on the temporal variations of concentration. As γ_1 increases, the only possible accompanying phenomenon is the decreasing of D_1 , since other parameters are held constant. According to the traditional concept in a single-porosity medium, decreasing dispersion would lead to less tailing and late breakthrough. This seems to be the only case in Fig. 2 when γ_1 changes from 1 to 10. The remaining cases contradict the normal observation. In other words, a decrease of γ_1 results in

an increase in tailing. This unusual phenomenon is the result of the capacitance effect, as expounded by Mannhardt and Nasr-El-Din (1994). Indeed, an enhanced solute exchange between macropores and mesopores would restrict the local solute concentration (at a point) in reaching its maximum value, and as such lead to extended tailing. This response is aggravated when the ratio of γ_1 to γ_2 becomes quite large [e.g., ratio $(v_1 D_2 / (v_2 D_1)) = 10$] where the contribution of solute exchange becomes substantial. Interestingly, a variable concentration slope change is noted for this case at the initial breakthrough. This behavior may reflect the local replenishment of mass from the mesopores to the macropores when the storage of the macropores becomes exhausted. This type of slope change, demonstrated as a fluctuation on the profiles of the breakthrough curves, was observed experimentally by Neretnieks (1993). This unusual dispersive response is difficult to decipher in the transport modeling because the process may be overshadowed by the simultaneous convective process.

To further ensure that the behavior of the single-porosity model is different from that of the triple-porosity model subjected to different EPN γ , Fig. 3 depicts the breakthrough curves for the single-porosity model (refer to Table 1) with different γ . As expected in traditional transport modeling, a

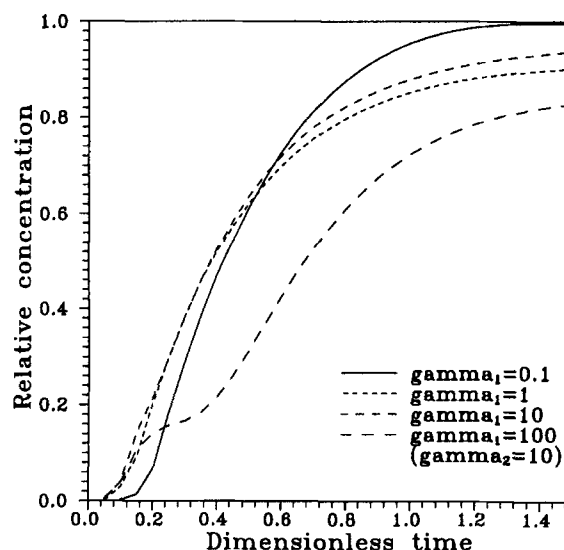


FIG. 2. Breakthrough Curves for Various EPNs of Macropores (γ_1)

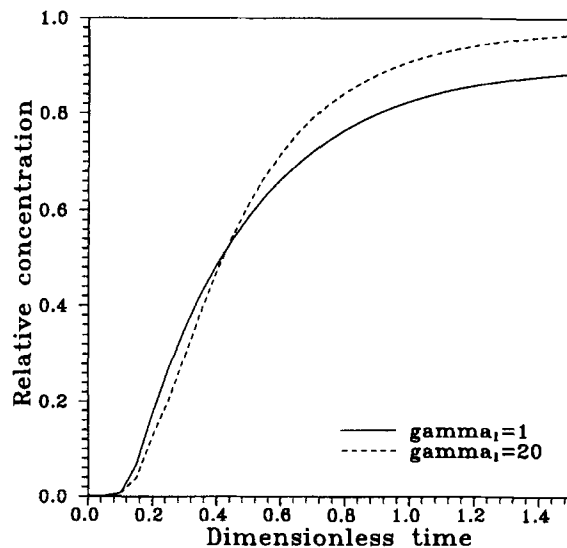


FIG. 3. Breakthrough Curves for Two EPNs of Macropores (γ_1)

smaller γ corresponds to earlier breakthrough and tailing, whereas the opposite is true for the larger γ .

Based on (10)–(12), the triple-porosity behavior is characterized by the magnitudes of the solute exchange intensity factor a_{ij} . For a fixed rate of solute exchange between the meso- and micropores, Fig. 4 describes temporal changes in concentration for varying exchange coefficients between the macro- and mesopores. Greater solute exchange between the larger pore regions appears to result in more rapid breakthrough with extended tailing, a typical feature for the multiporosity media. In contrast, less prominent solute exchange in the larger pore domains, which resembles the single-porosity response, shows a more regular Gaussian-type of breakthrough profile.

The velocity ratio b , between the micropores and mesopores provides a reasonable benchmark to evaluate the impact of flow velocity alone. Fig. 5 depicts significant differences in temporal concentration, when the velocity contrast between macro- and mesopores increases. The smaller velocity ratio ($b_2 = 2$) signifies less-dominant transport within the macropores, but a more significant influence from the mass exchange between macropores and mesopores, leading to an early breakthrough and extended tailing. With the increase of the velocity ratios (equivalent to the decrease of v_2 since v_1 is fixed), the dominance of macropore transport becomes increasingly apparent, which results in the progressively delayed but convective-

tion-controlled breakthrough curves, an indication of the increasing velocity contrast between the main flow region and the less permeable regions. Similar phenomena have been observed experimentally by McKibbin (1985), Houseworth (1988), and Bouhroum and Bai (1996). The velocity contrast is attributed to the permeability contrast among the different pore phases. The convective component becomes dominant as the permeability contrast increases.

The previous calculation does not consider the strong effects from the sorption process because the relatively small equivalent sorption intensity factors (ESIF) are used. With the increased magnitudes of ESIF in macropores, Fig. 6 reveals the significant differences in temporal concentrations, especially during the late evolution of the breakthrough curves. Different from the impact of interporosity mass exchange (as shown in Fig. 4), this retardation process, because of the enlargement of the macropore adsorption, results in the progressive tailing without the exhibition of apparent early abrupt breakthrough. Even though the solute exchange between the various porous spaces also creates retardation in the concentration changes, the differences between these two processes are that the retardation by fluid-solid sorption occurs primarily in the individual porous space (e.g., macropores), while the retardation by interporosity mass exchange occurs in the multiple porous spaces simultaneously. Consequently, the former process re-

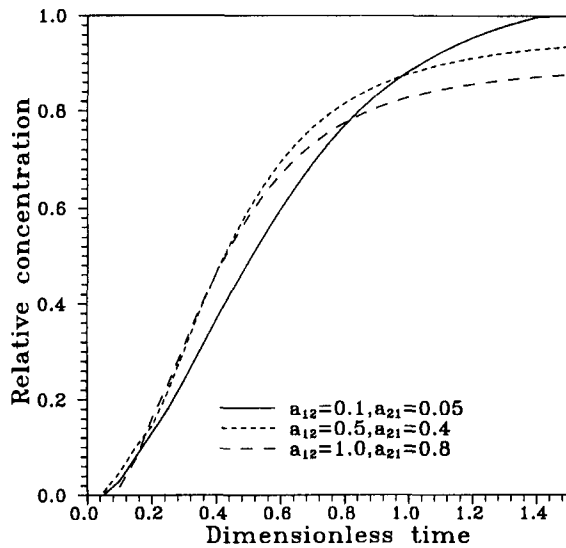


FIG. 4. Breakthrough Curves for Various Exchange Factors (a_{ij})

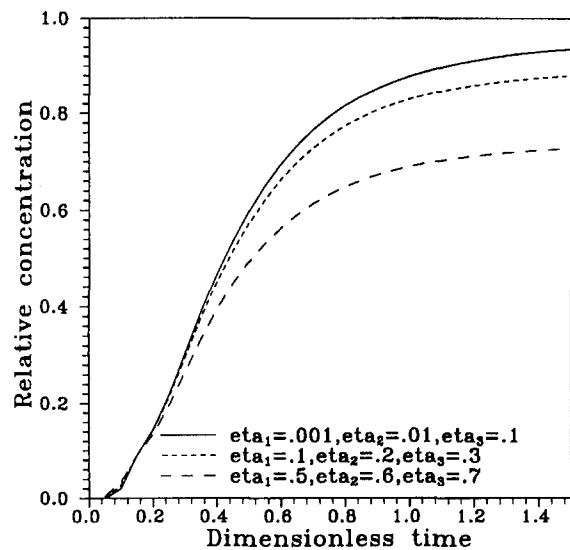


FIG. 6. Effect of Adsorption on Temporal Concentration

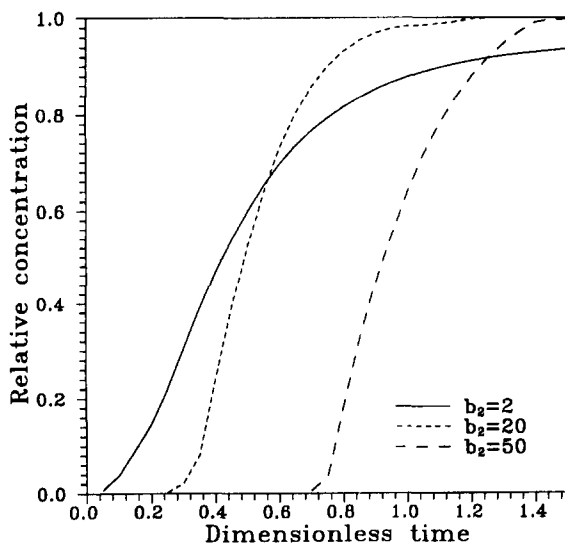


FIG. 5. Breakthrough Curves for Various Velocity Ratios (b)

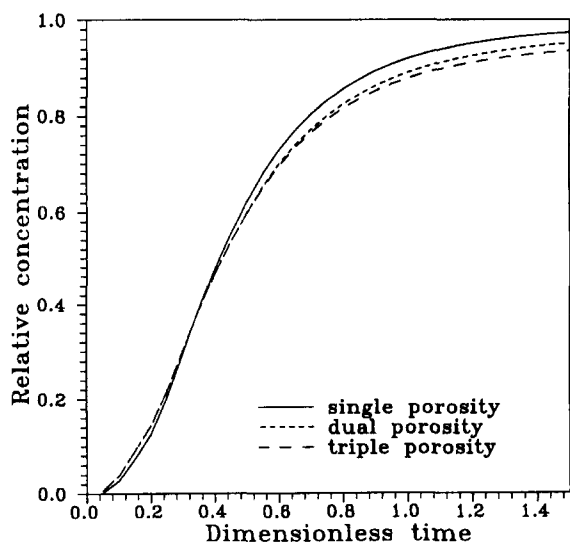


FIG. 7. Comparison of Temporal Concentration

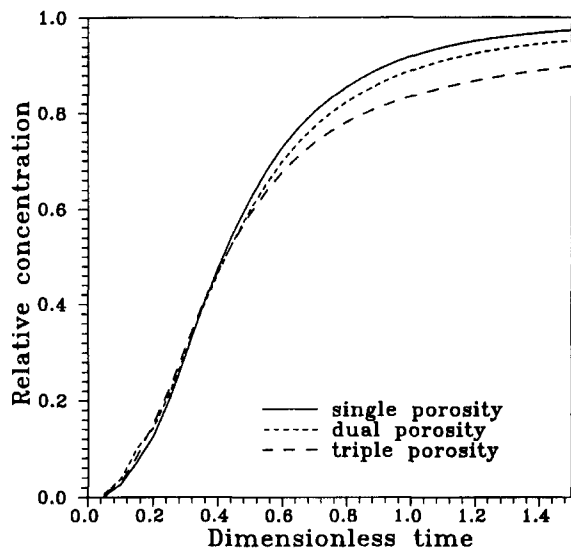


FIG. 8. Comparison of Temporal Concentration with Larger Exchange Rate

sults in direct concentration modification, such as a reduction in concentration (Fig. 6), as opposed to indirect time-dependent changes in concentration such as abrupt breakthroughs evident in the latter process (Fig. 4). The retardation effect by sorption was verified by Ogata (1964).

By manipulating the pertinent parameters in (10)–(12), a comparison of temporal concentrations can be made between single-porosity ($a_{12} = 0$), dual-porosity ($a_{23} = a_{32} = 0$), and triple-porosity models as shown in Fig. 7. Early breakthrough (slight in this case) and extended tailing are documented effects that index the level of transport heterogeneity and result from the interaction between preferential flow channels and less permeable regions. This behavior can be identified in both dual-porosity and triple-porosity models. Under the present set of parameters (Table 1), the differences between different models shown in Fig. 7 may be considered insignificant. However, incorporating more significant solute exchange rate between mesopores and micropores, the difference becomes more noticeable, as shown in Fig. 8.

CONCLUSIONS

Modeling solute migration in porous media with complex structure has primarily focused on simplified representation as two-region (dual-porosity) transport where the mass advected in the main channels is modified by diffusive exchange with components sequestered and effectively immobilized within the porous matrix. For porous media with a refined structure, where both mobile and immobile regions (e.g., macro- and micropores) are affected by dispersion and convection in a buffer zone (e.g., mesopores), a more comprehensive three-region (triple-porosity) approach offers an advantage. The most valuable extension is in consistently and appropriately representing a continuous distribution of pore sizes as three discrete intervals. The extension to a finer subdivision of pore sizes is transparent. The extension to modeling the response of three component media is straightforward, but adequate representation of the convective term, with the attendant problems of numerical dispersion, oscillation about the front and under- and overshoot, remains present for all convection dominated processes. In addition, interporosity mass exchange is the primary process for solute retardation (or attenuation) in the traditional dual-porosity and triple-porosity models. The sorption process, occurring between fluid phase and inclusive solid particles, may constitute another crucial retardation phenomenon and is sometimes neglected in these models.

To remedy this current situation, semianalytical solutions are presented in this analysis to evaluate solute transport with linear sorption in triple-porosity media. These solutions provide more physical insights in the complex hydrogeological system while offering a more flexible tool in matching experimental results when the porous medium exhibits a characteristic transport response of highly heterogeneous media, including extended tailing and nonuniform breakthrough. Apart from the standard numerical inversion using Laplace transforms, the solutions appear complete and procedures are straightforward. Sensitivity analysis identifies the EPN γ_i , flow velocity ratio b_i , and the equivalent sorption intensity factor η_i as the most significant parameters. In view of γ_i , a substantial decrease of macropore dispersion would result in the aggravated tailing or variable slope changes in the breakthrough curve. With regard to b_i , an increased velocity contrast between larger pores and other smaller pores may lead to a convection-dominated transport with progressively delayed breakthrough. Envisioning η_i , the enhanced adsorption within macropores may result in a monotonic concentration reduction, occurring in a less time-dependent manner. Another influential parameter includes the solute exchange intensity factor a_{ij} , which may introduce increased disparity between single-, dual-, and triple-porosity models. The triple-porosity model presented in this work may be used to interpret the nonstandard transport response of certain highly heterogeneous porous media and provides a basis to validate numerical models that represent similarly complex physical systems.

ACKNOWLEDGMENTS

Support of the National Science Foundation and Oklahoma State and Industrial Consortium under contract EEC-9209619 and under the S/TUCRC program is gratefully acknowledged.

APPENDIX I. DERIVATION OF \bar{c}_1 AND \bar{c}_2

Solution Procedure

The method of differential operators (Mathematical Handbook 1979) is defined as

$$D^{\bar{n}}f(x_i) = \frac{d^{\bar{n}}f(x_i)}{dx_i^{\bar{n}}} \quad (39)$$

where i indexes an arbitrary variable; and \bar{n} = order of the differential equations.

The coupled equations (37) and (34) can be solved using (39) as

$$\left(\frac{D^2}{\gamma_1} - D - \phi_{11}\right) \bar{c}_1 + a_{12}\bar{c}_2 = \phi_{12} \quad (40)$$

$$\left(\frac{D^2}{\gamma_2} - D - \phi_{21}\right) \bar{c}_2 + a_{21}\bar{c}_1 = \phi_{22} \quad (41)$$

Solving (40) and (41) simultaneously, yields

$$\bar{c}_1 = \frac{1}{a_{21}} \left[\phi_{22} - \left(\frac{D^2}{\gamma_2} - D - \phi_{21}\right) \bar{c}_2 \right] \quad (42)$$

$$(D^4 + \theta_1 D^3 + \theta_2 D^2 + \theta_3 D + \theta_4) \bar{c}_2 = \theta_5 \quad (43)$$

where

$$\theta_1 = -(\gamma_1 + \gamma_2); \quad \theta_2 = -(\gamma_1\phi_{11} + \gamma_2\phi_{21} - \gamma_1\gamma_2) \quad (44a,b)$$

$$\theta_3 = \gamma_1\gamma_2(\phi_{11} + \phi_{21}); \quad \theta_4 = \gamma_1\gamma_2(\phi_{11}\phi_{21} - a_{12}a_{21}) \quad (44c,d)$$

$$\theta_5 = -\gamma_1\gamma_2(a_{21}\phi_{12} + \phi_{11}\phi_{22}) \quad (44e)$$

The solution \bar{c}_2 from (43) can be expressed as

$$\bar{c}_2 = \bar{c}_2^h + \bar{c}_2^p \quad (45)$$

where \bar{c}_2^h and \bar{c}_2^n = homogeneous and nonhomogeneous solutions, respectively; where \bar{c}_2^n can be derived as $\bar{c}_2^n = \theta_4^{-1}\theta_3$ or

$$\bar{c}_2 = \bar{c}_2^h + \theta_4^{-1}\theta_3, \quad (46)$$

For homogeneous solutions \bar{c}_2^h , the four roots from (43) can be derived in the following manner. Rewriting (43) as

$$D^2 + \xi_1 D + \phi_1 = 0, \quad D^2 + \xi_2 D + \phi_2 = 0 \quad (47)$$

where

$$\xi_1 = \frac{1}{2}(\theta_1 + \sqrt{\Delta_1}), \quad \xi_2 = \frac{1}{2}(\theta_1 - \sqrt{\Delta_1}) \quad (48a)$$

$$\phi_1 = z + \frac{\theta_1 z - \theta_3}{\sqrt{\Delta_1}}, \quad \phi_2 = z - \frac{\theta_1 z - \theta_3}{\sqrt{\Delta_1}} \quad (48b)$$

$$\Delta_1 = 8z + \theta_1^2 - 4\theta_2 \quad (48c)$$

and where z = any real root of the following equation:

$$8z^3 + 4E_1 z^2 + E_2 z + E_3 = 0 \quad (49)$$

and where

$$E_1 = -\theta_2, \quad E_2 = 2\theta_1\theta_3 - 8\theta_4, \quad E_3 = \theta_4(4\theta_2 - \theta_1^2) - \theta_3^2 \quad (50)$$

Further, assume $z = u - (E_1/6)$, where the parameter u can be determined from the third-order equation $u^3 + pu + q = 0$ and where

$$p = \frac{1}{8} \left(E_2 - \frac{2E_1^2}{3} \right), \quad q = \frac{1}{8} \left(\frac{2E_1^3}{27} - \frac{E_1 E_2}{6} + E_3 \right) \quad (51)$$

The three roots of u may be described as

$$u_1 = F_1 + F_2, \quad u_2 = \rho_1 F_1 + \rho_2 F_2, \quad u_3 = \rho_2 F_1 + \rho_1 F_2 \quad (52)$$

where

$$F_1 = \left(-\frac{q}{2} + \sqrt{\Delta^*} \right)^{1/3}, \quad F_2 = \left(-\frac{q}{2} - \sqrt{\Delta^*} \right)^{1/3} \quad (53a)$$

$$\rho_1 = -\frac{1}{2} + \frac{\sqrt{3}}{2}i, \quad \rho_2 = -\frac{1}{2} - \frac{\sqrt{3}}{2}i \quad (53b)$$

$$\Delta^* = \left(\frac{q}{2} \right)^2 + \left(\frac{p}{3} \right)^3 \quad (53c)$$

Three possible solutions of the real root z exist depending upon the signs of Δ^* in (53), as indicated by the magnitude of Δ^* .

When $\Delta^* > 0$, the real root is

$$z = F_1 + F_2 - \frac{E_1}{6} \quad (54)$$

If $\Delta^* = 0$, then the real root becomes

$$z = -\sqrt[3]{4q} - \frac{E_1}{6} \quad (55)$$

However, if $\Delta^* < 0$, the real root is recovered in trigonometric form as

$$z = 2\sqrt[3]{r} \cos \left(\frac{\alpha^*}{3} \right) - \frac{E_1}{6} \quad (56)$$

where

$$r = \sqrt{-\left(\frac{p}{3}\right)^3}, \quad \alpha^* = \arccos \left(-\frac{q}{2r} \right) \quad (57)$$

Once the real root z is determined for (49), the four roots of (43) can then be expressed as

$$\psi_1 = -\frac{\xi_1}{2} + \sqrt{\Delta_2}, \quad \psi_2 = -\frac{\xi_1}{2} - \sqrt{\Delta_2} \quad (58a)$$

$$\psi_3 = -\frac{\xi_2}{2} + \sqrt{\Delta_3}, \quad \psi_4 = -\frac{\xi_2}{2} - \sqrt{\Delta_3} \quad (58b)$$

$$\Delta_2 = \frac{\xi_1^2}{4} - \phi_1, \quad \Delta_3 = \frac{\xi_2^2}{4} - \phi_2 \quad (58c)$$

The solutions in the Laplace domain may become complicated as a result of uncertainty in the signs of Δ_1 , Δ_2 , and Δ_3 , which will be presented later.

Solving System of Equations

Following the previous analytical procedure, a system of equations can be established after satisfying boundary conditions as expounded in (23)

$$\begin{bmatrix} d_{11} & d_{12} & d_{13} & d_{14} \\ d_{21} & d_{22} & d_{23} & d_{24} \\ d_{31} & d_{32} & d_{33} & d_{34} \\ d_{41} & d_{42} & d_{43} & d_{44} \end{bmatrix} \begin{Bmatrix} g_1 \\ g_2 \\ g_3 \\ g_4 \end{Bmatrix} = \begin{Bmatrix} c_1^* \\ c_2^* \\ 0 \\ 0 \end{Bmatrix} \quad (59)$$

where

$$c_1^* = \phi_{22} + \phi_{21}\theta_4^{-1}\theta_3 - a_{21}\frac{c^0}{s}, \quad c_2^* = \frac{c^0}{s} - \theta_4^{-1}\theta_3 \quad (60)$$

Solutions of (59) can be expressed as

$$g_i = \frac{I_i}{J} \quad (i = 1, 2, 3, 4) \quad (61)$$

where

$$J = \sum_{i=1}^4 (-1)^{i-1} d_{1i} J_i \quad (62)$$

and where J_i can be described as

$$J_i = d_{2j}(d_{3k}d_{4l} - d_{4k}d_{3l}) - d_{2k}(d_{3j}d_{4l} - d_{4j}d_{3l}) + d_{2l}(d_{3j}d_{4k} - d_{4j}d_{3k}) \quad (63)$$

and it follows the rotation rule, i.e., $i \neq j \neq k \neq l$. More specifically

$$\begin{aligned} i = 1, \quad j = 2, \quad k = 3, \quad l = 4 \\ i = 2, \quad j = 3, \quad k = 4, \quad l = 1 \\ i = 3, \quad j = 4, \quad k = 1, \quad l = 2 \\ i = 4, \quad j = 1, \quad k = 2, \quad l = 3 \end{aligned} \quad (64)$$

Similarly

$$\begin{aligned} I_i = (-1)^i [(c_2^* d_{1j} - c_1^* d_{2j})(d_{3k} d_{4l} - d_{3l} d_{4k}) \\ - (c_2^* d_{1k} - c_1^* d_{2k})(d_{3j} d_{4l} - d_{3l} d_{4j}) \\ + (c_2^* d_{1l} - c_1^* d_{2l})(d_{3j} d_{4k} - d_{3k} d_{4j})] \end{aligned} \quad (65)$$

where the retrogressive rotation rule is applied, i.e.

$$\begin{aligned} i = 1, \quad j = 2, \quad k = 3, \quad l = 4 \\ i = 2, \quad j = 1, \quad k = 3, \quad l = 4 \\ i = 3, \quad j = 1, \quad k = 2, \quad l = 4 \\ i = 4, \quad j = 1, \quad k = 2, \quad l = 3 \end{aligned} \quad (66)$$

The solution procedure includes the derivation of \bar{c}_1 and \bar{c}_2 along with the components of the system matrix in (59), $d_{\beta i}$ ($\beta = 1, 2, 3, 4$ and $i = 1, 2, 3, 4$). The coefficients g_i ($i = 1,$

2, 3, 4) in the solutions can then be readily calculated from (61).

Analytical Solutions when $\Delta_1 \geq 0$

For $\Delta_1 \geq 0$, the solutions in the Laplace domain can be divided into four groups depending on the signs of Δ_2 and Δ_3 .

Case 1: $\Delta_2 \geq 0$ and $\Delta_3 \geq 0$

The solution from (43) and (46) can be written as

$$\bar{c}_2 = \sum_{i=1}^4 g_i e^{\psi_i y} + \theta_4^{-1} \theta_5 \quad (67)$$

$$\bar{c}_1 = \frac{1}{a_{21}} \left[\phi_{22} + \phi_{21} \theta_4^{-1} \theta_5 - \sum_{i=1}^4 g_i \Omega_{1i} e^{\psi_i y} \right] \quad (68)$$

where

$$\Omega_{1i} = \frac{\psi_i^2}{\gamma_2} - \psi_i - \phi_{21} \quad (69)$$

After satisfying boundary conditions in (23), $d_{\beta i}$ are derived as

$$d_{1i} = \Omega_{1i}, \quad d_{2i} = 1, \quad d_{3i} = \Omega_{3i}, \quad d_{4i} = \Omega_{2i}; \quad (i = 1, 2, 3, 4) \quad (70)$$

where

$$\Omega_{2i} = \psi_i e^{\psi_i}, \quad \Omega_{3i} = \Omega_{1i} \Omega_{2i} \quad (71)$$

Case 2: $\Delta_2 \geq 0$ and $\Delta_3 < 0$

$$\bar{c}_2 = \sum_{i=1}^2 g_i e^{\psi_i y} + e^{\omega_3 y} [g_3 \cos(\omega_4 y) + g_4 \sin(\omega_4 y)] + \theta_4^{-1} \theta_5 \quad (72)$$

where

$$\omega_3 = -\frac{\xi_2}{2}, \quad \omega_4 = \sqrt{-\Delta_3} \quad (73)$$

$$\bar{c}_1 = \frac{1}{a_{21}} \left(\phi_{22} + \phi_{21} \theta_4^{-1} \theta_5 - \sum_{i=1}^2 g_i \Omega_{1i} e^{\psi_i y} + e^{\omega_3 y} \{g_3 [\lambda_3 \cos(\omega_4 y) - \lambda_4 \sin(\omega_4 y)] + g_4 [\lambda_3 \sin(\omega_4 y) + \lambda_4 \cos(\omega_4 y)]\} \right) \quad (74)$$

where

$$\lambda_3 = \frac{1}{\gamma_2} (\omega_3^2 - \omega_4^2) - \omega_3 - \phi_{21}, \quad \lambda_4 = \omega_4 \left(\frac{2\omega_3}{\gamma_2} - 1 \right) \quad (75)$$

For $i = 1, 2$, $d_{\beta i}$ are identical to those in the case 1. However, for $i = 3, 4$

$$d_{1i} = \lambda_i, \quad d_{2i} = 1 \quad (i = 3), \quad d_{2i} = 0 \quad (i = 4) \quad (76a)$$

$$d_{33} = e^{\omega_3} [\lambda_3^* \cos(\omega_4) - \lambda_4^* \sin(\omega_4)],$$

$$d_{34} = e^{\omega_3} [\lambda_3^* \sin(\omega_4) + \lambda_4^* \cos(\omega_4)] \quad (76b)$$

$$d_{43} = e^{\omega_3} [\omega_3 \cos(\omega_4) - \omega_4 \sin(\omega_4)],$$

$$d_{44} = e^{\omega_3} [\omega_3 \sin(\omega_4) + \omega_4 \cos(\omega_4)] \quad (76c)$$

where

$$\lambda_3^* = \omega_3 \lambda_3 - \omega_4 \lambda_4, \quad \lambda_4^* = \omega_3 \lambda_4 + \omega_4 \lambda_3 \quad (77)$$

Case 3: $\Delta_2 < 0$ and $\Delta_3 \geq 0$

$$\bar{c}_2 = e^{\omega_1 y} [g_1 \cos(\omega_2 y) + g_2 \sin(\omega_2 y)] + \sum_{i=3}^4 g_i e^{\psi_i y} + \theta_4^{-1} \theta_5 \quad (78)$$

where

$$\omega_1 = -\frac{\xi_1}{2}, \quad \omega_2 = \sqrt{-\Delta_2} \quad (79)$$

$$\bar{c}_1 = \frac{1}{a_{21}} (\phi_{22} + \phi_{21} \theta_4^{-1} \theta_5 - e^{\omega_1 y} \{g_1 [\lambda_1 \cos(\omega_2 y) - \lambda_2 \sin(\omega_2 y)] + g_2 [\lambda_1 \sin(\omega_2 y) + \lambda_2 \cos(\omega_2 y)]\}) + \sum_{i=3}^4 g_i \Omega_{1i} e^{\psi_i y} \quad (80)$$

where

$$\lambda_1 = \frac{1}{\gamma_2} (\omega_1^2 - \omega_2^2) - \omega_1 - \phi_{21}, \quad \lambda_2 = \omega_2 \left(\frac{2\omega_1}{\gamma_2} - 1 \right) \quad (81)$$

For $i = 3, 4$, $d_{\beta i}$ are identical to those in the case 1. However, for $i = 1, 2$

$$d_{1i} = \lambda_i, \quad d_{2i} = 1 \quad (i = 1), \quad d_{2i} = 0 \quad (i = 2) \quad (82a)$$

$$d_{31} = e^{\omega_1} [\lambda_1^* \cos(\omega_2) - \lambda_2^* \sin(\omega_2)],$$

$$d_{32} = e^{\omega_1} [\lambda_1^* \sin(\omega_2) + \lambda_2^* \cos(\omega_2)] \quad (82b)$$

$$d_{41} = e^{\omega_1} [\omega_1 \cos(\omega_2) - \omega_2 \sin(\omega_2)],$$

$$d_{42} = e^{\omega_1} [\omega_1 \sin(\omega_2) + \omega_2 \cos(\omega_2)] \quad (82c)$$

where

$$\lambda_1^* = \omega_1 \lambda_1 - \omega_2 \lambda_2, \quad \lambda_2^* = \omega_1 \lambda_2 + \omega_2 \lambda_1 \quad (83)$$

Case 4: $\Delta_2 < 0$ and $\Delta_3 < 0$

$$\bar{c}_2 = e^{\omega_1 y} [g_1 \cos(\omega_2 y) + g_2 \sin(\omega_2 y)] + e^{\omega_3 y} [g_3 \cos(\omega_4 y) + g_4 \sin(\omega_4 y)] + \theta_4^{-1} \theta_5 \quad (84)$$

$$\bar{c}_1 = \frac{1}{a_{21}} (\phi_{22} + \phi_{21} \theta_4^{-1} \theta_5 - e^{\omega_1 y} \{g_1 [\lambda_1 \cos(\omega_2 y) - \lambda_2 \sin(\omega_2 y)] + g_2 [\lambda_1 \sin(\omega_2 y) + \lambda_2 \cos(\omega_2 y)]\} + e^{\omega_3 y} \{g_3 [\lambda_3 \cos(\omega_4 y) - \lambda_4 \sin(\omega_4 y)] + g_4 [\lambda_3 \sin(\omega_4 y) + \lambda_4 \cos(\omega_4 y)]\}) \quad (85)$$

$d_{\beta i}$ can be expressed as

$$d_{1i} = \lambda_i, \quad (i = 1, 2, 3, 4), \quad d_{2i} = 1, \quad (i = 1, 3);$$

$$d_{2i} = 0, \quad (i = 2, 4) \quad (86a)$$

$$d_{31} = e^{\omega_1} [\lambda_1^* \cos(\omega_2) - \lambda_2^* \sin(\omega_2)],$$

$$d_{32} = e^{\omega_1} [\lambda_1^* \sin(\omega_2) + \lambda_2^* \cos(\omega_2)] \quad (86b)$$

$$d_{33} = e^{\omega_3} [\lambda_3^* \cos(\omega_4) - \lambda_4^* \sin(\omega_4)],$$

$$d_{34} = e^{\omega_3} [\lambda_3^* \sin(\omega_4) + \lambda_4^* \cos(\omega_4)] \quad (86c)$$

$$d_{41} = e^{\omega_1} [\omega_1 \cos(\omega_2) - \omega_2 \sin(\omega_2)],$$

$$d_{42} = e^{\omega_1} [\omega_1 \sin(\omega_2) + \omega_2 \cos(\omega_2)] \quad (86d)$$

$$d_{43} = e^{\omega_3} [\omega_3 \cos(\omega_4) - \omega_4 \sin(\omega_4)],$$

$$d_{44} = e^{\omega_3} [\omega_3 \sin(\omega_4) + \omega_4 \cos(\omega_4)] \quad (86e)$$

All the parameters have been defined in the previous cases.

Analytical Solutions when $\Delta_1 < 0$

If $\Delta_1 < 0$, then ξ_1 , ξ_2 , ϕ_1 , and ϕ_2 in (48) become complex variables. It is not necessary, as in the previous cases, to determine the signs for Δ_2 and Δ_3 , which are redefined as

$$\Delta_2 = \Omega_1 + i\Omega_2, \quad \Delta_3 = \Omega_1 - i\Omega_2 \quad (87)$$

where

$$\Omega_1 = \frac{1}{16}(\theta_1^2 + \Delta_1) - z, \quad \Omega_2 = \frac{\theta_1}{8} \sqrt{-\Delta_1} + \frac{\theta_1 z - \theta_3}{\sqrt{-\Delta_1}} \quad (88)$$

Δ_2 and Δ_3 need to be expressed in trigonometric forms, which imply dual set of solutions. For the first set of solutions, the corresponding four roots in (58) can be written as

$$\psi_1 = \omega_1^* + i\omega_2^*, \quad \psi_2 = \omega_3^* - i\omega_4^* \quad (89a)$$

$$\psi_3 = \omega_1^* - i\omega_2^*, \quad \psi_4 = \omega_3^* + i\omega_4^* \quad (89b)$$

where

$$\omega_1^* = \sqrt{r^*} \cos\left(\frac{\theta^*}{2}\right) - 0.25\theta_1, \quad \omega_2^* = \sqrt{r^*} \sin\left(\frac{\theta^*}{2}\right) - 0.25\sqrt{-\Delta_1} \quad (90a)$$

$$\omega_3^* = -\left[\sqrt{r^*} \cos\left(\frac{\theta^*}{2}\right) + 0.25\theta_1\right], \quad \omega_4^* = \sqrt{r^*} \sin\left(\frac{\theta^*}{2}\right) + 0.25\sqrt{-\Delta_1} \quad (90b)$$

$$\sqrt{r^*} = \sqrt{\Omega_1^2 + \Omega_2^2}, \quad \theta^* = \arctan\left(\frac{\Omega_2}{\Omega_1}\right) \quad (90c)$$

The solutions can be derived as

$$\bar{c}_2 = e^{\omega_1^* y} [g_1 \cos(\omega_2^* y) + g_3 \sin(\omega_2^* y)] + e^{\omega_3^* y} [g_2 \sin(\omega_4^* y) + g_4 \cos(\omega_4^* y)] + \theta_4^{-1} \theta_5 \quad (91)$$

$$\bar{c}_1 = \frac{1}{a_{21}} \{ \phi_{22} + \phi_{21} \theta_4^{-1} \theta_5 - g_1 e^{\omega_1^* y} [\alpha_{11} \cos(\omega_2^* y) + \alpha_{12} \sin(\omega_2^* y)] + g_2 e^{\omega_3^* y} [\alpha_{21} \sin(\omega_4^* y) + \alpha_{22} \cos(\omega_4^* y)] + g_3 e^{\omega_1^* y} [\alpha_{31} \sin(\omega_2^* y) + \alpha_{32} \cos(\omega_2^* y)] + g_4 e^{\omega_3^* y} [\alpha_{41} \cos(\omega_4^* y) + \alpha_{42} \sin(\omega_4^* y)] \} \quad (92)$$

where

$$\alpha_{11} = \frac{1}{\gamma_2} [(\omega_1^*)^2 - (\omega_2^*)^2] - \omega_1^* - \phi_{21}, \quad \alpha_{12} = \omega_2^* \left(1 - \frac{2\omega_1^*}{\gamma_2}\right) \quad (93a)$$

$$\alpha_{21} = \frac{1}{\gamma_2} [(\omega_3^*)^2 - (\omega_4^*)^2] - \omega_3^* - \phi_{21}, \quad \alpha_{22} = -\omega_4^* \left(1 - \frac{2\omega_3^*}{\gamma_2}\right) \quad (93b)$$

$$\alpha_{31} = \alpha_{11}, \quad \alpha_{32} = -\alpha_{12}, \quad \alpha_{41} = \alpha_{21}, \quad \alpha_{42} = -\alpha_{22} \quad (93c)$$

For (59), $d_{\beta i}$ can be expressed as

$$d_{1i} = \alpha_{11}, \alpha_{22}, \alpha_{32}, \alpha_{41}, \quad (i = 1, 2, 3, 4) \quad (94a)$$

$$d_{2i} = 1, \quad (i = 1, 4), \quad d_{2i} = 0, \quad (i = 2, 3) \quad (94b)$$

$$d_{31} = e^{\omega_1^* y} [\alpha_{11}^* \cos(\omega_2^* y) + \alpha_{12}^* \sin(\omega_2^* y)],$$

$$d_{32} = e^{\omega_3^* y} [\alpha_{21}^* \sin(\omega_4^* y) + \alpha_{22}^* \cos(\omega_4^* y)] \quad (94c)$$

$$d_{33} = e^{\omega_1^* y} [\alpha_{31}^* \sin(\omega_2^* y) + \alpha_{32}^* \cos(\omega_2^* y)],$$

$$d_{34} = e^{\omega_3^* y} [\alpha_{41}^* \cos(\omega_4^* y) + \alpha_{42}^* \sin(\omega_4^* y)] \quad (94d)$$

$$d_{41} = e^{\omega_1^* y} [\omega_1^* \cos(\omega_2^* y) - \omega_2^* \sin(\omega_2^* y)],$$

$$d_{42} = e^{\omega_3^* y} [\omega_3^* \sin(\omega_4^* y) + \omega_4^* \cos(\omega_4^* y)] \quad (94e)$$

$$d_{43} = e^{\omega_1^* y} [\omega_1^* \sin(\omega_2^* y) + \omega_2^* \cos(\omega_2^* y)],$$

$$d_{44} = e^{\omega_3^* y} [\omega_3^* \cos(\omega_4^* y) - \omega_4^* \sin(\omega_4^* y)] \quad (94f)$$

where

$$\alpha_{11}^* = \omega_1^* \alpha_{11} + \omega_2^* \alpha_{12}, \quad \alpha_{12}^* = \omega_1^* \alpha_{12} - \omega_2^* \alpha_{11} \quad (95a)$$

$$\alpha_{21}^* = \omega_3^* \alpha_{21} - \omega_4^* \alpha_{22}, \quad \alpha_{22}^* = \omega_3^* \alpha_{22} + \omega_4^* \alpha_{21} \quad (95b)$$

$$\alpha_{31}^* = \omega_1^* \alpha_{31} - \omega_2^* \alpha_{32}, \quad \alpha_{32}^* = \omega_1^* \alpha_{32} + \omega_2^* \alpha_{31} \quad (95c)$$

$$\alpha_{41}^* = \omega_3^* \alpha_{41} + \omega_4^* \alpha_{42}, \quad \alpha_{42}^* = \omega_3^* \alpha_{42} - \omega_4^* \alpha_{41} \quad (95d)$$

For the second set of solutions when $\Delta_1 < 0$, simply substitute $\cos(\theta^*/2)$ with $\cos[(\theta^*/2) + \pi]$ and substitute $\sin(\theta^*/2)$ with $\sin[(\theta^*/2) + \pi]$.

APPENDIX II. REFERENCES

- Abdassah, D., and Ershaghi, I. (1986). "Triple-porosity system for representing naturally fractured reservoirs." *Soc. Petroleum Engrg. J.*, 281(4), 113-127.
- Anderson, M. P. (1979). "Using models to simulate the movement of contaminants through ground water flow systems." *Critical Rev. in Environ. Control*, 9, 97-156.
- Bai, M., and Elsworth, D. (1995). "On the modeling of miscible flow in multi-component porous media." *Transp. in Porous Media*, 21(1), 19-46.
- Bai, M., Elsworth, D., and Roegiers, J.-C. (1993). "Multi-porosity/multi-permeability approach to the simulation of naturally fractured reservoirs." *Water Resour. Res.*, 29(6), 1621-1633.
- Bai, M., Roegiers, J.-C., and Inyang, H. I. (1996). "Contaminant transport in nonisothermal fractured porous media." *J. Envir. Engrg., ASCE*, 122(5), 416-423.
- Barenblatt, G. I., Zheltov, I. P., and Kochina, N. (1960). "Basic concepts in the theory of seepage of homogeneous liquids in fissured rocks." *Prikl. Mat. Mekh.*, 24(5), 852-864.
- Bear, J. (1972). *Dynamics of fluids in porous media*. Elsevier, New York, N.Y.
- Bouhroum, A., and Bai, M. (1996). "Experimental and numerical simulation of solute transport in heterogeneous porous media." *Int. J. Numer. and Analytical Methods Geomech.*, 20, 155-171.
- Brusseau, M. L., and Rao, P. S. C. (1990). "Modelling solute transport in structured soils: a review." *Geoderma*, 46, 169-192.
- Chen, Z.-X. (1989). "Transient flow of slightly compressible fluids through double-porosity, double-permeability systems—a state of the art review." *Transp. in Porous Media*, 4, 147-184.
- Coats, K. H., and Smith, B. D. (1964). "Dead-end pore volume and dispersion in porous media." *Soc. Petroleum Engrg. J.*, 4(3), 73-84.
- Gerke, H. H., and van Genuchten, M. T. (1993). "A dual-porosity model for simulating the preferential movement of water and solutes in structured porous media." *Water Resour. Res.*, 29(2), 305-319.
- Gwo, J. P., Jardine, P. M., Wilson, G. V., and Yeh, G. T. (1995). "A multiple-pore-region concept to modeling mass transfer in subsurface media." *J. Hydro.*, 164, 217-237.
- Gwo, J. P., Jardine, P. M., Wilson, G. V., and Yeh, G. T. (1996). "Using a multiregion model to study the effects of advective and diffusive mass transfer on local physical nonequilibrium and solute mobility in a structured soil." *Water Resour. Res.*, 32(3), 561-570.
- Houseworth, J. E. (1988). "Characterizing permeability heterogeneity in core samples from standard miscible displacement experiments, SPE 18329." *Proc., 63rd Society of Petroleum Engineer Annual Tech. Conf. and Exhib.*, Houston, Tex.
- Li, L., Barry, D. A., Culligan-Hensley, P. J. and Bajracharya, K. (1994). "Mass transfer in soils with local stratification of hydraulic conductivity." *Water Resour. Res.*, 30(11), 2891-2900.
- Luxmoore, R. J., Jardine, P. M., Wilson, G. V., Jones, J. R., and Zelazny, L. W. (1990). "Physical and chemical controls of preferred path flow through a forest hillslope." *Geoderma*, 46, 139-154.
- Mannhardt, K., and Nasr-El-Din, H. A. (1994). "A review of one-dimen-

sional convection-dispersion models and their applications to miscible displacement in porous media." *In Situ*, 18(3), 277-345.

Mathematical handbook. (1979). People's Education Publishing Company, Beijing, China (in Chinese).

McKibbin, R. (1985). "Thermal convection in layered and anisotropic porous media: a review." *Proc., CSIRO/DSIR Seminar on Convective Flows in Porous Media*, Wellington, New Zealand, 113-127.

Neretnieks, I. (1993). "Solute transport in fractured rock—applications to radionuclide waste repositories." *Flow and contaminant transport in fractured rock*, J. Bear, et al., eds., Academic Press, Inc., San Diego, Calif., 39-128.

Ogata, A. (1964). "Mathematics of dispersion with linear adsorption isotherm." *Geological professional paper, 411-H*, U.S. Government Printing Office, Washington, D.C.

Passioura, J. B. (1971). "Hydrodynamic dispersion in aggregated media. 1: theory." *Soil Sci. Soc. Am. Proc.*, 111(6), 339-344.

Stehfest, H. (1970). "Algorithm 358—numerical inversion of Laplace transforms." *Comm. of ACM*, 13(1), 47-49.

Warren, J. E., and Root, P. J. (1963). "The behavior of naturally fractured reservoirs." *Soc. Petroleum Engrg. J.*, 3, 245-255.

Water Science and Technology Board (WSTB). (1990). *Ground water models, scientific and regulatory applications*. National Academy Press, Washington, D.C.

APPENDIX III. NOTATION

The following symbols are used in this paper:

- a = solute exchange intensity factor;
- b = velocity ratio;

- c = solute concentration;
- c^0 = concentration at the source;
- c_i^0 = initial concentration in the i pore space;
- c^* = dimensionless concentration;
- D = hydrodynamic dispersion;
- L = length of contaminant migration;
- K_p = sorption intensity factor;
- n = porosity;
- s = Laplace parameter;
- t = time;
- v = average fluid flow velocity;
- x = linear distance from source;
- y = dimensionless distance;
- γ = equivalent Péclet number (EPN);
- ϵ = process factor;
- η = equivalent sorption intensity factor;
- ξ = concentration exchange coefficient;
- σ = function of sorption isotherm;
- σ_i^0 = initial sorbent concentration in the i pore space;
- σ^* = dimensionless sorbent concentration; and
- τ = dimensionless time.

Subscripts

- 1 = macropores;
- 2 = mesopores; and
- 3 = micropores.

Copyright of Journal of Environmental Engineering is the property of American Society of Civil Engineers and its content may not be copied or emailed to multiple sites or posted to a listserv without the copyright holder's express written permission. However, users may print, download, or email articles for individual use.